Charging of Large Structures in Space with Application to the Solar Sail Spacecraft

Jay R. Hill and Elden C. Whipple Jr.
University of California at San Diego, La Jolla, California

Some Important Charging Effects at Low Altitudes

Introduction

THE ionosphere as a rule is a rather benign environment as far as charging of spacecraft is concerned. The ionospheric plasma is relatively cool and dense in comparison with other plasmas in space. The plasma density ranges from values on the order of 10^6 cm^{-3} to values as low as or even below 10^2 cm^{-3}, with temperatures well below 1 eV (11,600 K). However, there can be large fluxes of energetic electrons in the polar ionosphere. The possibility that these auroral fluxes could charge a spacecraft to large potentials makes this subject a matter of concern. However, even moderate charging of spacecraft can complicate the interpretation of data from scientific experiments on satellites in the ionosphere.

Figures 1 and 2 show how two important length scales vary in the ionosphere. Figure 1 shows that the Debye length ranges from about 1 mm to a few centimeters. The electrostatic sheath thickness about a charged object is on the order of a few Debye lengths. Thus, in the ionosphere, the Debye length is very small compared to a large space structure. Figure 2 shows typical electron and proton gyroradii in the ionosphere. Again, the electron gyroradius is small, on the order of a few centimeters to 1 m. The proton gyroradius is larger, up to tens of meters in size, and thus can be comparable to the dimensions of large space structures.

The charging of objects in the ionosphere is characterized by extreme anisotropy in the charging currents. The ion current is dominated by the motion of the spacecraft in its motion through the plasma and hence the ion current occurs largely on the leading surfaces of such an object. The electron current does not vary as strongly as the ion current but is affected by the $\bar{V}\times\bar{B}$ and wake effects which cause it to also vary with position on the spacecraft surface. The photoemission current varies with surface orientation with respect to sunlight.

Possibility of Large Potentials in the Polar Ionosphere

Katz and Park[1] studied the possible charging effects of large electron fluxes in the auroral ionosphere on a spacecraft. They took an energetic electron flux of 2×10^{-4} A/m^2 at an energy of 3 keV and examined its effect on an orbiting sphere in the ionospheric plasma with a density of 10^5 cm^{-3} at a temperature of about 0.1 eV. In their model, the large negative current due to the energetic electrons was balanced primarily by the positive current due to ion collection. The significant result obtained by Katz and Parks was that the sphere would charge to large negative potentials approaching the energy of the auroral electrons. This occurred because the increase in ion current necessary to balance the electron current was limited by the sheath thickness. The sheath thickness grows slowly with the potential drop across the sheath when the Debye length is small and, hence, a large potential drop is required to obtain the necessary ion current.

This result is illustrated in Fig. 3 which shows how the equilibrium potential of the sphere increases with its radius. In regions where the plasma concentration is small, the potentials are correspondingly greater. A more precise calculation must include secondary electron currents and photoemission but, in principle, it is possible to have large potentials in regions where large energetic electron fluxes occur. It is important to know the frequency of occurrence of large fluxes of energetic electrons in the polar ionosphere.

The Wake Effect

The plasma wake behind a moving body is a region depleted unequally of both ions and electrons because of the small thermal velocities of the ions compared to the streaming velocity. Electrons can readily penetrate this region until the negative space charge from the excess electrons builds up the negative

Jay R. Hill was born in 1944 in Fullerton, California. He received a B.S. in physics from Loma Linda University in 1966 and a Ph.D. in applied physics from the University of California at San Diego in 1981. He is presently employed at SAIC and UCSD. Dr. Hill has published several papers investigating the physical and dynamical processes of charged dust within planetary and cometary environments including dust charging, electrostatic disruption, trajectories and distribution of charged dust in the environments near comets and in the magnetospheres of Jupiter and Saturn.

Elden C. Whipple Jr. was born in 1931 in Bellingham, Washington. He received his B.S. in physics at Wheaton College in 1955, and M.S. and Ph.D. degrees in physics at the George Washington University in Washington, D.C. in 1958 and 1965. He carried out research in atmospheric electricity at the Naval Research Laboratory, Washington, D.C. from 1956 to 1958. In 1958 he joined NASA's Goddard Space Flight Center and worked with a group making the first direct measurements of ionospheric quantities by satellite. He continued ionospheric and magnetospheric research with the Aeronomy Laboratory of the National Oceanic and Atmospheric Administration in Boulder, Colorado, from 1965 to 1975. In 1975 Dr. Whipple joined the University of California at San Diego, where he is currently research physicist and Associate Director of the Center for Astrophysics and Space Sciences. His fields of research include the physics of the upper atmosphere and magnetosphere, plasma physics, and especially the problem of the interactions between space vehicles and the surrounding plasma.

Received Oct. 19, 1984; revision received Jan. 21, 1985.

potential to a value such that they are depleted as well. This acts as a negative potential barrier for electron collection on the rear surfaces of the spacecraft.

Figure 4 (from Ref. 2) shows how the electron current measured on Explorer 31 varied with angle, with 0 deg corresponding to the ram direction. The electron current at lower altitudes is depleted by as much as two orders of magnitude on the back surface compared to the front surface, with smaller depletions at higher altitudes. The back-to-front current ratio is shown in Fig. 5 as a function of the mean ion mass. The altitude dependence of the current vs angle curves of Fig. 4 is in reality a dependence on the mean ion mass which decreases with altitude, as the dominant ion changes from oxygen to helium and then to hydrogen.

It is difficult to calculate the height of this negative potential barrier in the wake which controls the rear-surface electron current, although Samir's data show that it varies linearly with the square of the ion Mach number.[3] The barrier also depends on the Debye length.

Another effect of the wake is that insulating portions of a body in the wake may charge to large negative potentials. Parker[4] has calculated potential contours around an insulating cylinder immersed in a streaming plasma, with an ion Mach number equal to 4. The rear surface charges to a potential that is more than an order of magnitude larger than (kT/e). However, Parks and Katz[5] have shown that rotation of the body can reduce the magnitude of the rear-surface potentials because of the "spin current" associated with the charge carried around by the rotation.

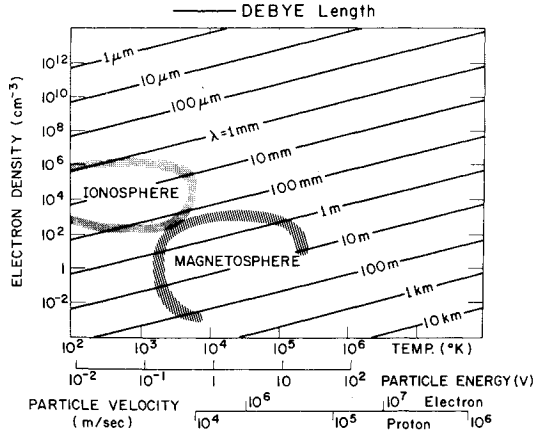

Fig. 1 Debye length as a function of plasma density and temperature.

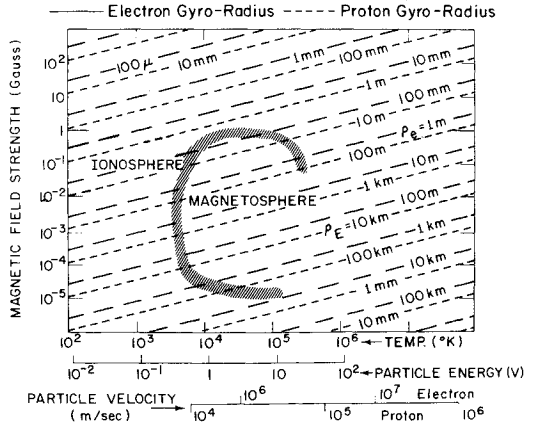

Fig. 2 Electron and proton gyroradius.

The $\vec{V}\times\vec{B}$ Effect

A body moving across a magnetic field experiences an electric field given by $\vec{V}\times\vec{B}$. In the reference frame of the moving body this is a real electric field which interacts with a conducting body by inducing electric charges at the body's surface. This is illustrated in Fig. 6 which shows such a body moving in the ionosphere. The electric field in the region of space around the body is indicated by the equipotential contours. At a great distance from the body, the equipotential contours are straight, indicating a uniform electric field, but in the body's vicinity the contours are distorted by the conductor's presence. The conducting body itself is at a given potential, but the potential difference between the body and the adjacent plasma depends on the position at which the potential difference is taken. This variation in potential difference occurs

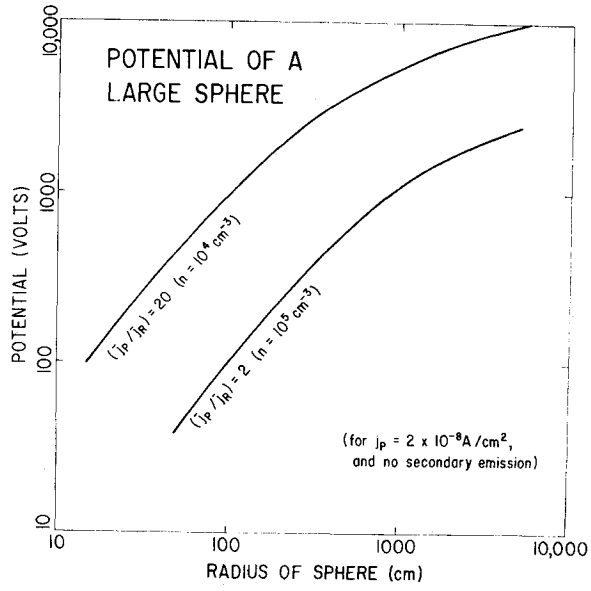

Fig. 3 Potential of a large sphere vs sphere radius in the auroral ionosphere with an incident current of energetic electrons.

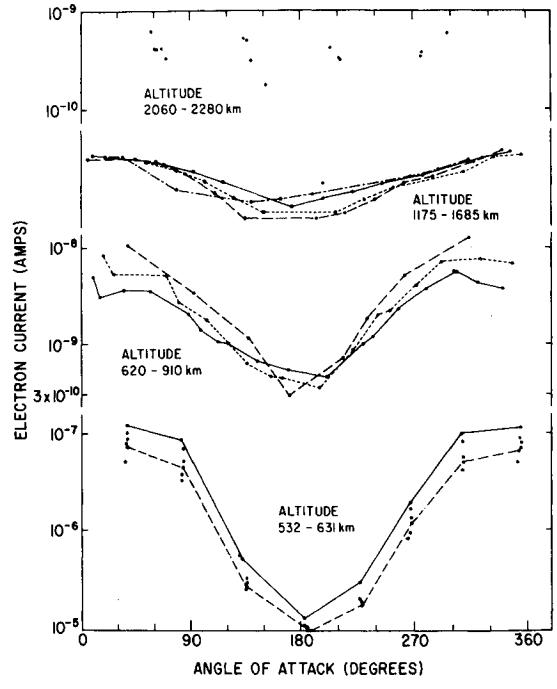

Fig. 4 Electron current vs angle of attack from Explorer 31, from Ref. 2.

not because the body potential varies, but because the reference potential in the adjacent plasma is varying with position.

Since the current collected by a surface in a plasma depends on the potential difference with respect to the plasma, it follows that the current density to the body will vary with position on the body's surface. The end of the body that is more positive with respect to the adjacent plasma will tend to collect electrons, whereas the negative end will collect ions. Since the electron current density is higher than the ion current density for a given potential difference due to the smaller mass of the electron, the current balance condition which determines the equilibrium potential will drive the body to a potential so that only a small area will be at a positive potential with respect to the adjacent plasma, as illustrated in Fig. 6.

The variation in collected current to such a body means that a current flows along the body from the negative to the positive end, as illustrated in Fig. 7. In equilibrium, this current path must close through the plasma. There has been almost no work on the problem of how this current returns through the plasma. The current loop must disturb the plasma, with the disturbance being proportionately greater for larger structures. It is important to understand this interaction and to know how the distant plasma responds to the presence of a large structure.

Electron Collection for Large Positive Potentials

The mechanism for electron collection by moderately or highly positively charged moving bodies in the ionosphere is not well understood. However, some data on this question have been obtained from electron beam emission experiments carried on vehicles in the ionosphere.[6] The plasma response to electron beam emission experiments appears to be quite different in the ionosphere than in the low-density magnetosphere. Both ion and electron beam experiments have been carried out in the magnetosphere on the ATS-5, ATS-6, and SCATHA satellites.[7] There has been no evidence of any kind of a beam plasma discharge (BPD) in these beam emission experiments at synchronous altitudes.

Cohen[8] has shown that charging a vehicle by ion beam emission in the ionosphere is consistent with the return current consisting of ions collected from the ionospheric plasma. However, electron beam experiments in the ionosphere have yielded vehicle potentials much lower than the beam energy.[6,9] (A possible exception is the results of Jacobson and Maynard.)[10] Anomalously high return electron currents have kept vehicle potentials low. A BPD may have occurred in some of these experiments, but the evidence of this is not yet convincing, although the data showed that there were a large number of heated electrons in the vicinity of the vehicle. These heated electrons were produced by a variety of processes, probably including collisional ionization of the ambient and vehicle-produced neutral gases, secondary electron production, and the effects of waves and instabilities excited in the surrounding plasma.

The asymptotic behavior for the plasma around a body moving throught a magnetized plasma is not known. Parker and Murphy[11] discussed the motion of electrons in the plasma about a charged sphere and showed that the electron gyrocenters would themselves drift in a spiral about the body. Linson[12] argued that turbulent diffusion would enable the electrons to cross the magnetic field lines. Figure 8 (from Ref. 12) shows the variation of collected electron current vs potential on a charged sphere under various assumptions. The upper curve is an upper limit based on the Langmuir-Blodgett[13] sheath approximation. The lower curve represents the currents derived from the work of Parker and Murphy.[11] The intermediate curves represent the possible effects of turbulence in increasing the collected current. The parameter q_c is the critical value of the ratio of the square of the plasma frequency to the electron gyrofrequency. At a value of this parameter on the order of unity, the plasma is unstable to the growth of turbulence.

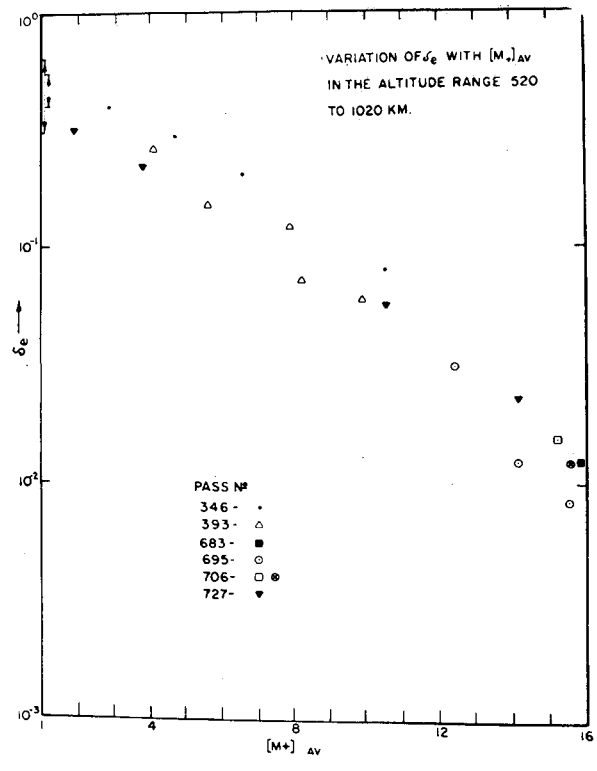

Fig. 5 The back-to-front electron current ratio vs mean ion mass, from Explorer 31.[25]

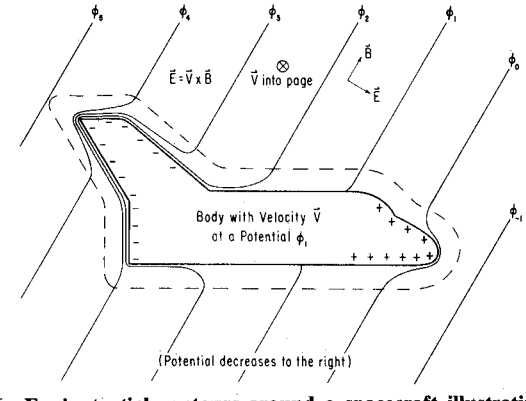

Fig. 6 Equipotential contours around a spacecraft illustrating the $\vec{V}\times\vec{B}$ effect.

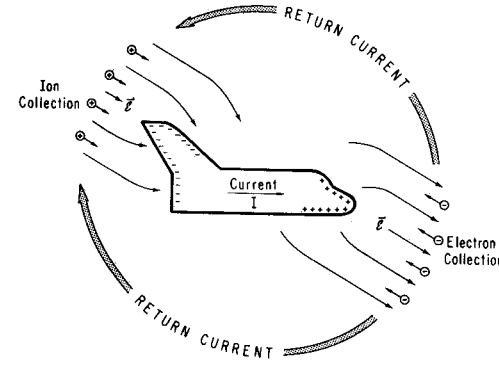

Fig. 7 The problem of the return current path around a spacecraft where the $\vec{V}\times\vec{B}$ effect occurs.

Charging of the Solar Sail in Earth Orbit

Geometry of the Solar Sail

An experimental solar sail spacecraft is being designed and built for launch into Earth orbit in the near future. The general objective is to evaluate solar sailing technology and to gain experience in the design and operation of a solar sail vehicle. The sail will be deployed from the vehicle when the spacecraft is in an orbit with perigee at about 1200 km and apogee at geosynchronous altitude of about 36,000 km. During each orbit, the sail will be turned relative to the sun to maximize the perigee altitude gain during the orbit.

The sail will have a 1000-2000 m^2 area supported by four spars extending from the spacecraft body, as shown in Fig. 9. The basic structure of the spacecraft will be aluminum alloy. Spars will be fabricated from stainless steel or a composite material such as fiberglass/epoxy. The sail will be an aluminized plastic film of approximately 0.5-mil-thick Mylar or Kapton. The four sail corners will be attached to the spar tips for deployment.

A study has been made of the electrodynamics of charged particle interactions with a square sail 30 m on each side. The study calculated the effects of all reasonable sources of charged particles as they affect the total charge on the sail and spacecraft. The equilibrium potential of the sail was determined as a function of altitude. The following sections describe the environmental model, the currents to the sail, and the resulting potentials.

Model of the Environment

The environment is characterized by a relatively cool and dense plasma at low altitudes inside the Earth's plasmasphere and by a relatively hot and rarefied plasma outside the Earth's plasmasphere. A simple exponential fit to the ion density at the lower altitudes[14] has been chosen.

$$n = 10^{(15-L)/3.5} \tag{1}$$

Where L denotes the magnetic shell whose equatorial radius is L Earth radii. The boundary to the plasmasphere in Earth radii has been fit by

$$L = 9.913\ (Ap)^{-0.1955} \tag{2}$$

where (Ap) is the index of magnetic activity. The Ap index is a quasilinear daily index of geomagnetic activity, the average of eight 3-h Ap values which are transformations of the 3-h quasilogarithmic Kp index. The Kp index[15] is based on magnetic observations at 13 high-latitude stations. A single curve was fit to the temperature profile[16,17]:

$$T(\text{eV}) = 0.09293\ L^{2.70173} \tag{3}$$

When the temperature of the plasma given by Eq. (3) is greater than 1 eV, the plasma is considered to have two components: the hot one with T given by Eq. (3) and density $n = 1$ cm^{-3}. The cold portion has $T = 1$ eV with a density 1 cm^{-3} less than in Eq. (1).

In the plasmasphere the sail's orbit velocity (calculated on the basis of an assumed circular orbit at a given altitude) relative to the corotating plasma in centimeters per second is

$$v = 100(GM/r^{1/2} - r\,\Omega) \tag{4}$$

where $GM = 398.603 \times 10^{12}$ m^3/s^2, $\Omega = 7.292115 \times 10^{-5}$ rad/s, r is the Earth-sail distance in meters. Outside the plasmasphere the plasma is assumed to be stationary so that $\Omega = 0$.

The authors have chosen to use the extensive data available from the ATS-5 and ATS-6 satellites in geosynchronous orbit for the outer magnetosphere. There are two models for the plasma in this region. One is the worst-case (highest-energy) model[18] and the other a standard condition model[19] with two parameters: local time and the magnetic activity index, Ap. The worst-case plasma conditions, shown in Table 1, are listed in the two-Maxwellian plasma model. The hot and cold ion and electron component densities and temperatures were derived from measurements of the first four moments of the velocity distributions.

Plasma Currents to the Sail

The equilibrium potential on the sail is achieved when all of the currents to the sail are in balance. The time required to reach equilibrium in a given plasma environment depends on the size of the object being charged. Micrometeors in the magnetosphere of Jupiter, for example, take hours to become charged to equilibrium potential.[20,21] On the other hand, spacecraft in the Earth's magnetosphere need only milliseconds.[3] Thus the solar sail will always be very close to equilibrium potential (the time constant is about 2-100 ms) and we need only concern ourselves here with the current balance equation.

$$I_{\text{net}} = I_i + I_e + I_{\text{se}} + I_{\text{si}} + I_b + I_p = 0 \tag{5}$$

where I_i is the ion current, I_e the electron current, I_{se} the secondary electron current from electron impact, I_{si} the secondary electron current from ion impact, I_b the backdiffusion electron current, and I_p the photoelectron current.

Each of these currents is a function of the potential of the sail, so that the solution of Eq. (5) requires an iterative evaluation. Multiple solutions of Eq. (5) are possible[3] when the secondary electron emission becomes large as a result of covering the satellite with certain dielectrics. However, this should

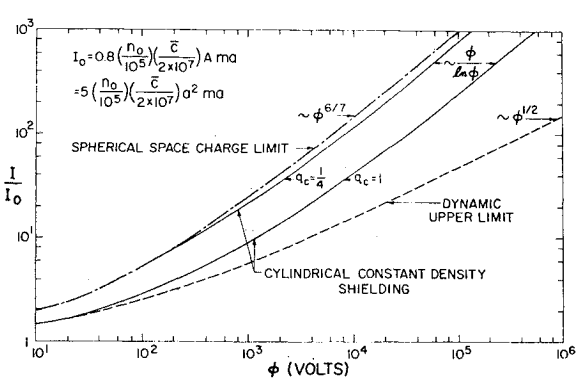

Fig. 8 Possible current/voltage relationships for a sphere with a large positive potential in the ionosphere (from Ref. 12).

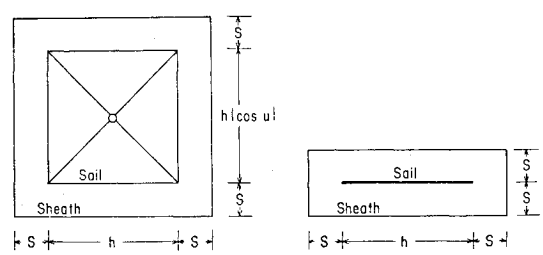

Fig. 9 Geometry of the solar sail.

Table 1 Worst-case plasma components

Component	Cold	Hot
N_e, cm^{-3}	0.2	1.45
T_e, eV	400	24,400
N_i, cm^{-3}	1.35	1.45
T_i, eV	300	27,100

not occur with an aluminum surface such as that on the solar sail. The current equations for spheres, infinite cylinders, and planes in a stationary plasma are relatively simple compared to those for the sail because of its size, shape, and motion through the plasma. A discussion of these and other effects, including sheath thickness and wake effects on the current equations, follows in the remainder of this section.

Ion Current

A useful approximation for the ion current in a repulsive field and moving plasma is

$$I_i = Anqv\,[1-2V/mv^2]\cos u, \qquad 0<V<mv^2/2q \tag{6}$$

as long as the ion thermal motion can be neglected. Here A is the area, v the velocity of the body relative to the plasma, u the angle between v and the normal to A, n the ion density, q the ion charge, m the ion mass, and V the potential on the spacecraft. When

$$V>mv^2/2q \tag{7}$$

the current is essentially zero. Now if we use the Kepler velocity at a distance r from the Earth's center for v then Eq. (7) becomes

$$V>GMm/2qr=0.3262/L \tag{8}$$

so that at geosynchronous orbit Eq. (6) will be valid for $0<V<0.05$ V. For larger positive potentials the current will not be zero, since the ion thermal motion will provide some current:

$$I_i = 2Anqv_{\text{ion}}\exp(-Vq/kT)/(2\pi^{1/2}) \tag{9}$$

where

$$v_{\text{ion}}^2 = 2kT/m_{\text{ion}} \tag{10}$$

The attractive ion current is complicated by the existence of a sheath surrounding the spacecraft which increases its effective size. The relation between the ion current outside the sheath and the sheath thickness S [Ref. 22, Eq. (15)] is

$$S^4 = (2q/m)V^3/(81\pi^2J^2) \tag{11}$$

The current density J is the sum of the current components (hot or cold electrons), each of which is given by[23]

$$J_j = n_jRAM_jT_j^{1/2}$$

where

$$RAM_j = \exp(-M_j^2) + \pi^{1/2}\,[M_j + M_j\text{erf}(M_j)\,]$$

and the Mach number is obtained from

$$M_j^2 = (m_jv^2/2kT_j)\cos^2 u \tag{12}$$

The following equation for the ion current to the sail moving in a plasma is correct in the limits of very small or large Debye length or the spacecraft speed much larger or smaller than the ion thermal speed. It has similarities to Eq. (3.4) of Ref. 24 and Eq. (4.4) of Ref. 3 but with the spherical spacecraft area replaced by the cross section and total surface areas of the sail including the sheath (see Fig. 9). The volume flow rates P and Q are weighted "means" of bulk and thermal flow rates multiplied by the appropriate surface area. The subscript c refers to the cross-sectional area and s the sheath surface area. The current for ions with temperature T_j is

$$I_j = n_jq\{Q-P\exp[(Q/P-1)V/T_j]\} \tag{13}$$

where P and Q have units of area × velocity,

$$Q = Q_cv\,\text{erf}\,x + Q_sv_{\text{ion}}\,[(\text{erf}\,x)/(8x) + \exp(-x^2)/(4\pi^{1/2})\,]$$

$$P = P_cv\,\text{erf}\,x + P_sv_{\text{ion}}\,[(\text{erf}\,x)/(8x) + \exp(-x^2)/(4\pi^{1/2})\,] \tag{13a}$$

and

$$Q_c = (2S+h)(2S+h\,|\cos u\,|), \qquad Q_s = 2(2S+h)^2$$

$$P_c = 2S[2S+h(1+\,|\cos u\,|)\,], \qquad P_s = 8S(S+h) \tag{13b}$$

with $x = v/v_{\text{ion}}$, and h the width of the square sail (see Fig. 9).

Electron Current

Wake effects make it difficult to determine the electron current to the back side of the sail. First, the front side current is considered. The current is simply the random electron flux to the sheath area when $V>0$.

$$I_f = -n_jq(h+2S)^2v_e/(2\pi^{1/2}) \qquad V>0$$

$$= -n_jqAv_e\exp\{qV/kT_j\}/(2\pi^{1/2}) \qquad V<0 \tag{14}$$

where

$$v_e^2 = 2kT_e/m_e \tag{15}$$

For the back side electron current with the wake effect,[3] first a plasma with only a single Maxwellian component is considered. To zeroth order, the relation between the front and back currents is

$$I_b = I_f\exp(-\,|\cos u\,|qW/kT) \qquad V<0$$

where the effective potential barrier W in the wake[3,25] is obtained from

$$qW/kT = -0.7-0.19mv^2/2kT \tag{16}$$

Since W depends on the Debye length λ, the (negative) potential in the wake[26] is limited by

$$(qW/kT)_{\max} = -2\ell n(h/\lambda) \tag{17}$$

In a multitemperature plasma, the Debye length, in centimeters, is

$$\lambda = 743\,[n_{\text{eh}}/T_{\text{eh}} + n_{\text{ec}}/T_{\text{ec}}\,]^{-1/2}$$

where *eh* refers to the hot component and *ec* to the cold electron component. Since the Debye length is fundamental in the wake effect, it is useful to use it to define an effective T for use

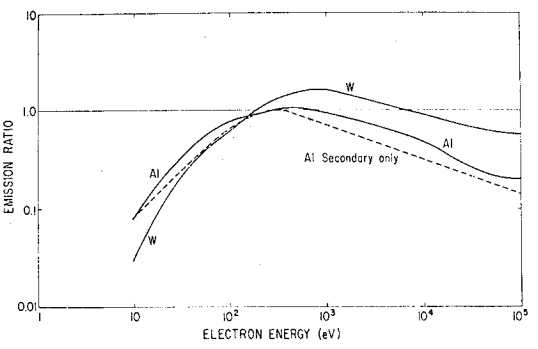

Fig. 10 Electron back-diffusion coefficients for aluminum and tungsten.

in Eqs. (16) and (17). That is,

$$T_{\text{eff}} = (n_{el}+n_{e2})/(n_{el}/T_{el}+n_{e2}/T_{e2}) \tag{18}$$

The total electron current is then

$$I_e = I_f[1+e^{-w}] \qquad V<0 \tag{19a}$$

where $w=(qW/kT)\,|\cos u|$, with (qW/kT) chosen as the least negative of Eqs. (16) and (17) using T from Eq. (18). When the potential is positive but not sufficiently to completely overcome the barrier potential, there is a mixture of attractive and repulsive fields.

$$I_e = I_f\{1+[h^2/(h+2S)^2]\exp(V/T-w)\}$$

$$0<V<-W|\cos u| \tag{19b}$$

When the potentials is sufficiently positive to completely overcome the barrier potential the electron current is

$$I_e = I_f[1+h^2/(h+2S)^2] \quad 0<-W|\cos u|<V \tag{19c}$$

Secondary and Photoemission Currents to the Sail

Back-Diffusion Current (Backscatter Current)

When electrons impact a surface there is a certain probability that they will not stick, but be reflected back as back-diffused primaries. Figure 10 (Ref. 24, p. 46) shows the back-diffusion coefficient for tungsten and aluminum. The coefficient has been modeled as a ramp from a value of zero at an energy E_1 to K_1 at an energy E_2. Figure 11 shows the back-diffusion coefficient determined by subtracting the best-fit secondary electron yield from the total reflected yield (Ref. 24, p. 47). The corresponding back-diffusion constants to be used in Eq. (21) are $K_1=0.24$, $E_1=280$ eV, and $E_2=500$ eV for aluminum. The constants for tungsten are $K_1=0.29$, $E_1=470$ eV, and $E_2=1000$ eV. When $V<0$, the normalized current is found from the integral

$$\frac{I_B}{I_e} = \int_{E_1}^{\infty} K(E)f(E)E\,dE \qquad V<0 \tag{20}$$

where $f(E)$ is the incident distribution at the surface. If $f(E)$ is a shifted Maxwellian, the result is

$$\frac{I_B}{I_e} = \frac{K_1}{[E_2/T-E_1/T]}\,[(2+E_1/T)e^{-E_1/T} - (2+E_2/T)e^{-E_2/T}] \tag{21}$$

When $V>0$, the back-diffusion current is found from

$$I_B = q\int_{qV}^{\infty} f_B(E)E\,dE \qquad V>0 \tag{22}$$

where the backscatter distribution function is approximately

$$f_B(E) = 2\int_E^{\infty} K(E')f(E')\,dE'/E' \qquad V<0 \tag{23}$$

For positive potentials when the Debye length is large, the small body formulas for the primary spectrum $f(E')$ are used. A ramp approximation is used for the yield function from $E=E_1$ to E_2 and $0<qV<E_1$.

$$I_B = Kn_e qAv_e e^{qV/kT}\pi^{-1/2}\,\frac{[F(E_2/kT)-F(E_1/kT)]}{[E_2/kT-E_1/kT]}$$

$$0<qV<E_1 \tag{24}$$

where the function $F(x)$ is

$$F(x) = [(qV/kT)^2-x-2]e^{-x} - (qV/kT)^2 xE_1(x) \tag{25}$$

and $E_1(x)$ is the exponential integral in Eq. (25) only.

Secondary Electron Current for Electron Impact

Secondary electrons can result from collisions of incident electrons with electrons within the material. The secondary yield has been determined[27] as a function of incident angle and energy E (see Ref. 3). Let $\bar{d}(E)$ be the angle averaged yield and

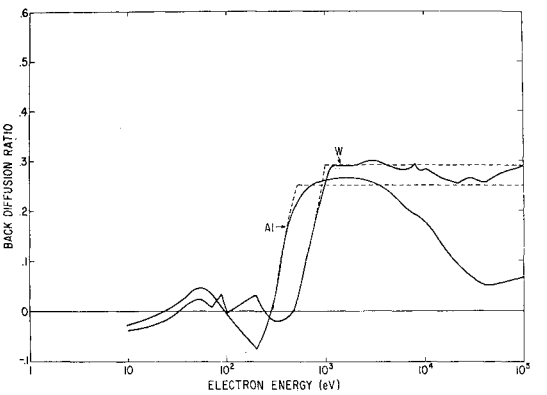

Fig. 11 Back-diffusion cofficients determined by subtracting the best fit secondary electron yield from the total reflected yield.

Table 2 Potential vs altitude and local hour angle. Garrett model for geosynchronous orbit, $Ap=32$

Hour angle, deg	Sail angle, deg	Altitude, km				
		9,567	15,945	22,324	28,702	35,080
0	−45	−1.981	−1.353	−0.713	5.257	5.257
30	−30	−1.786	−1.190	−0.565	5.626	5.626
60	−15	−1.733	−1.133	−0.505	5.813	5.813
90	0	−1.717	−1.116	−0.487	5.854	5.854
120	15	−1.733	−1.133	−0.505	5.759	5.759
150	30	−1.786	−1.190	−0.565	5.518	5.518
180	270	−3.935	−3.968	−4.009	−848.058	−848.192
210	60	−2.106	−1.541	−0.935	4.405	4.405
240	75	−2.528	−2.021	−1.453	3.151	3.151
270	90	−3.724	−3.696	−3.694	−1,801.087	−1,800.972
300	105	−2.528	−2.021	−1.453	3.114	3.114
330	120	−2.106	−1.541	−0.935	4.326	4.326

Table 3 Potential vs altitude and local hour angle. Garrett model for geosynchronous orbit, $Ap = 1056$

Hour angle, deg	Sail angle, deg	Altitude, km				
		9,567	15,945	22,324	28,702	35,080
0	−45	−1.981	0.001	0.001	0.001	0.001
30	−30	−1.786	0.219	0.219	0.219	0.219
60	−15	−1.733	0.372	0.372	0.372	0.372
90	0	−1.717	0.419	0.419	0.419	0.419
120	15	−1.733	0.365	0.365	0.365	0.365
150	30	−1.786	0.206	0.206	0.206	0.206
180	270	−3.935	−2,860.654	−2,860.753	−2,860.815	−2,860.858
210	60	−2.106	−146.154	−146.155	−146.155	−146.155
240	75	−2.528	−1,098.230	−1,098.230	−1,098.230	−1,098.230
270	90	−3.724	−3,492.127	−3,492.095	−3,492.074	−3,492.059
300	105	−2.528	−1,108.949	−1,108.949	−1,108.949	−1,108.949
360	120	−2.106	−125.536	−125.536	−125.537	−125.537

Table 4 Potential vs altitude and local hour angle. Worst-case model for geosynchronous orbit, $Ap = 1056$

Hour angle, deg	Sail angle, deg	Altitude, km				
		9,567	15,945	22,324	28,702	35,080
0	−45	−1.981	2.752	2.752	2.751	2.751
30	−30	−1.786	3.153	3.153	3.153	3.153
60	−15	−1.733	3.371	3.371	3.371	3.371
90	0	−1.717	3.440	3.440	3.440	3.440
120	15	−1.733	3.371	3.371	3.371	3.371
150	30	−1.786	3.153	3.153	3.153	3.153
180	270	−3.935	−10,342.817	−10,343.295	−10,343.598	−10,343.809
210	60	−2.106	2.076	2.075	2.075	2.075
240	75	−2.528	0.839	0.839	0.839	0.839
270	90	−3.724	−17,728.348	−17,728.012	−17,727.798	−17,727.650
300	105	−2.528	0.839	0.839	0.839	0.839
330	120	−2.106	2.076	2.075	2.075	2.075

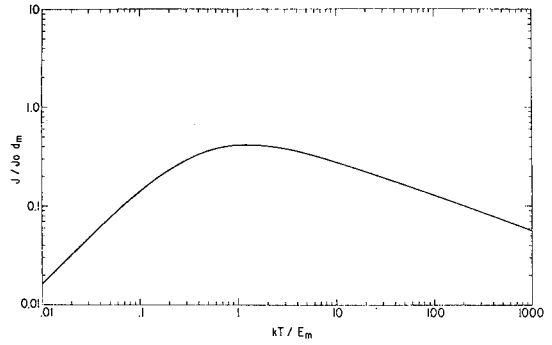

Fig. 12 The normalized back-diffusion current [from Eq. (29)].

$f(E)$ the distribution function of the incident electron energies. Then the secondary electron current is

$$I_s = (2Aq/m_e^2)\int_0^\infty \mathrm{d}(E) f(E) E \mathrm{d}E \tag{26}$$

where

$$\mathrm{d}(E) = 2.228(d_m/Q)(E_m/E)^{0.35}(Q - 1 + e^{-Q}) \tag{27}$$

where the quantity Q is defined by

$$Q = 2.28(E/E_m)^{1.35} \tag{28}$$

The secondary electron current constants for aluminum are $E_m = 230$ and $d_m = 1.0$. For tungsten, they are $E_m = 500$ and $d_m = 1.47$. Equation (26) can be integrated in an infinite series involving the gamma function $\Gamma(x)$. The result has two forms: one which converges for small values of $t = E_m/T$, the other for large values. Fortunately, the convergence regions of the two forms overlap. However, one must use Euler's transformation[28] to accelerate the convergence in the overlap region.

The integration of Eq. (26) is accomplished by expanding part of the exponential and evaluating term by term. The result involves a series of gamma functions. To aid in writing the solution $a = 2.228$ and $b = 2.28$ are used for the constants in Eqs. (27) and (28).

$$I_b/I_e = d_m(at^2/\pi)[\Gamma(33/20)t^{-33/20} - \Gamma(3/10)t^{-3/10}/b + S(t/b^{20/27})/b^{11/9}] \tag{29}$$

where $S(x)$ is a series

$$S(x) = 20/27 \sum_{k=0}^{\infty} (-x)^k \Gamma((20k+6)/27)/k! \qquad x < 2.5 \tag{30a}$$

$$S(x) = x^{-3/10} \sum_{k=0}^{\infty} (-1)^k x^{-27k/20} \Gamma((27k+6)/20)/k! \qquad x \geq 2.5 \tag{30b}$$

The first two terms in Eq. (30b) cancel the first two in Eq. (26) exactly, so that in the limit of $T << Em$ Eq. (26) is proportional to T. In the other limit, $T >> E_m$, using Eq. (30a), Eq. (26) is proportional to the $-7/20$ power of T. Since Eq. (26)

has a maximum value of 0.41 (see Fig. 12), there will always be a unique equilibrium potential. When d_m for the satellite material is greater than $1/0.41 = 2.44$, it becomes possible to have multiple solutions to the current balance equation[3,24] when the temperature of one of the plasma components is near E_m. The back-diffusion current will allow multiple solutions for T slightly greater than E_m. The back-diffusion ratio for aluminum is only 0.038 when $T = E_m$. Thus, aluminum is a factor of $2.23 = 1/(0.41 + 0.038)$ below the multiple solution condition.

Secondary Electron Current on Ion Impact

The secondary electron yield from proton impact[3,27] is approximately

$$Y(E) = 2Y_m (E/E_m)^{1/2}/(1 + E/E_m) \tag{31}$$

where Y_m is the maximum yield at an energy E_m. The current is

$$I_{si} = 2\pi A q/M^2 \int_0^\infty Y(E) f(E) E dE \qquad V < 0 \tag{32}$$

In the limit of a small body in a plasma with a Maxwellian energy distribution, we have

$$I_{si} = 2\pi^{-1/2} Y_m A q n_i v_{\text{ion}} e^{qV/kT} G(E_m/kT) \qquad V < 0 \tag{33}$$

where

$$G(x) = x^{1/2} \int_0^\infty u^{3/2} e^{-u} (x + u)^{-1} du$$

$$= (\pi x)^{1/2} (1 - 2x)/2 - \pi x^2 e^x \operatorname{erfc}(x^{1/2})$$

The potential dependence of the secondary electron current from ion impact must be equal to the ion current [Eq. (13)] when the yield is put to unity even when the electron distribution is not Maxwellian. This is approximated by

$$I_{si} = I_i Y_m G(E_m/kT) \qquad v_{\text{ion}} >> v_{\text{sail}} \tag{33a}$$

and when ion thermal motion is ignorable, use

$$I_{si} = I_i Y(0.5 m_i v_{\text{sail}}^2 - qV) \qquad v_{\text{ion}} << v_{\text{sail}} \tag{33b}$$

When $E_m >> kT$ is satisfied, the asymptotic formula $G(x) = 0.75(\pi/x)^{1/2}$ is useful. For aluminum, the constants are $E_m = 40$keV, $Y_m = 4.3$ (Ref. 3). Using these, we find the secondary yield is more than unity when $T > 3500$ eV. The yield peaks at 2.00876 when $T = 64$ keV and decreases slowly for yet higher energies. The ion energies in the *worst-case* model are high enough that the total secondary electron yield from ion impact reduces the potential to $-17{,}728$ V. Potentials of $-19{,}000$ V have been observed on ATS-6.

Photoelectron Current

Photoelectrons are those emitted when sunlight strikes a surface. The current for these electrons on aluminum is

$$I_p = 4.8 \times 10^{-9} A \, |\cos u| \qquad V < 0 \tag{34}$$

where A is the sunlit area in square centimeters. If the spacecraft potential is positive, some of the photoelectrons do not escape. An additional factor is required.

$$I_p = 4.8 \times 10^{-9} A \, |\cos u| e^{-V/T} \qquad V > 0 \tag{35}$$

where T is the photoelectron temperature, about 2 eV. In the Earth's shadow the photoelectron current is reduced by six orders of magnitude from the sunlit value.

Equilibrium Sail Potentials

The potentials on the solar sail as a function of location (altitude and local time) have been determined from the preceding model. Table 2 shows the sail potential when $Ap = 32$ and Table 3 when $Ap = 1056$. The worst-case plasma conditions were used to predict the maximum potentials shown in Table 4. The potential is small and negative inside the plasmasphere, and small and positive above it, except when the sail is in the Earth's shadow, where it is large and negative. The altitude of the plasmasphere is a function of Ap at $L = 5.0$ when $Ap = 32$ and at $L = 2.5$ when $Ap = 1056$.

The extreme potentials can be avoided completely if the shadow can be avoided while the sail is outside the plasmasphere. This can be accomplished if the orbital inclination i were at least $\arcsin(1/L)$, where L is the apogee in Earth radii, and the orbit were oriented so that the apogee were away from the sun. This requires $i > 12$ deg for $Ap = 32$ and $i > 24$ deg for $Ap = 1056$.

Extreme potentials can occur on the sail when the sail moves edgewise into the plasma. In this condition, the ion current is a minimum. If at the same time the sail is also in the Earth's shadow or placed edgewise to the sunlight, a large negative potential is possible. The exact calculation of the potential for these "edgewise" configurations is difficult. The result ($-10{,}000$ V) are highly dependent upon the details of the (at best) approximate calculation.

Acknowledgments

The authors acknowledge helpful discussions with H.B. Garrett. This work was partially supported by the California Space Institute.

References

[1]Katz, I. and Parks, D.E., "Space Shuttle Orbiter Charging," AIAA Paper 82-0119, *20th Aerospace Sciences Meeting*, Jan. 1982.

[2]Samir, U., and Wrenn, G.L. "The Dependence of Charge and Potential Distribution Around a Spacecraft on Ionic Composition," *Planetary and Space Science*, Vol. 17, 1969, p. 693.

[3]Whipple, E.C., "Potentials of Surfaces in Space," *Reports on Progress in Physies. Prog. Phys.*, Vol. 44, 1981, p. 114.

[4]Parker, L.W., "Differential Charging and Sheath Asymmetry of Nonconducting Spacecraft Due to Plasma Flows," *Journal of Geophysical Research*, Vol. 83, 1978, p. 4873.

[5]Parks, D.E. and Katz, I.J., "Mechanisms that Limit Potentials on Ionospheric Satellites," *Journal of Geophysical Research*, Vol. 88, 1983, p. 9155.

[6]Winckler, J.R., "The Application of Artificial Electron Beams to Magnetospheric Research," *Reviews of Geophysic and Space Physics*, Vol. 18, 1980, p. 659.

[7]Olsen, R.C., "Experiments in Charge Control, ATS-5 and ATS-6," *Journal of Spacecraft and Rockets*, Vol. 22, May-June 1985, pp. 254-264.

[8]Cohen, H.A., Sherman, C., and Mullen, E.G., "Spacecraft Charging Due to Positive Ion Emission: An Experimental Study," *Geophysical Research Letters*, Vol. 6, 1979, p. 515.

[9]Arnoldy, R.L., Winckler, J.R., "The Hot Plasma Environment and Floating Potentials of an Electron-Beam-Emitting Rocket in the Ionosphere," *Journal of Geophysical Research*, Vol. 86, 1981, p. 575.

[10]Jacobson, T.A. and Maynard, N.D., "Polar 5—An Electron Accelerator Experiment Within an Aurora. 3. Evidence for Significant Spacecraft Charging by an Electron Accelerator at Ionospheric Altitudes," *Planetary and Space Science*, Vol. 28, 1980, p. 291.

[11]Parker, L.W. and Murphy, B.L., "Potential Buildup on an Electron Emitting Ionospheric Satellite," *Journal of Geophysical Research*, Vol. 72, 1967, p. 1631.

[12]Linson, L.M., "Current-Voltage Characteristics of an Electron Emitting Satellite in the Ionosphere," *Journal of Geophysical Research*, Vol. 74, 1969, p. 2368.

[13]Langmuir, I. and Blodgett, K., "Currents Limited by Space Charge Between Concentric Spheres," *Physical Review*, Vol. 24, 1924, p. 49.

[14]Banks, P.M. and Kockarts, G., *Aeronomy*, Academic Press, New York, 1973.

[15]Rostoker, G., "Geomagnetic Indices," *Reviews of Geophysics and Space Physics*, Vol. 10, 1972, p. 935.

[16]Willmore, A.P., "Electron and Ion Temperatures in the Ionosphere," *Space Science Reviews*, Vol. 11, 1970, p. 607.

[17]Allen, C.W., *Astrophysical Quantities,* The Athlone Press, London, 1976.
[18]Mullen, E.G., Gussenhoven, M.S., and Garrett, H.B., "A Worst Case Spacecraft Charging Environment as Observed by SCATHA on 24 April 1979," AFGL-TR-81-0231, 1981.
[19]Garrett, H.B. and DeForest, S.E., "An Analytical Simulation of the Geosynchronous Plasma Environment," *Planetary and Space Sciences,* Vol. 27, 1979, p. 1101.
[20]Hill, J.R. and Mendis, D.A., "Charged Dust in Outer Planetary Magnetospheres: I. Physical and Dynamical Processes," *Moon and Planets*, Vol. 21, 1979, p. 3.
[21]Hill, J.R. and Mendis, D.A., "Charged Dust in the Outer Planetary Magnetospheres: II. Trajectories and Spatial Distribution," *Moon and Planets*, Vol. 23, 1980, p. 53.
[22]Garrett, H.B., "The Charging of Spacecraft Surfaces," *Reviews of Geophysics and Space Physics,* Vol. 19, 1981, p. 577.
[23]Parker, L.W., "Plasmasheath-Photosheath Theory for Large High-Voltage Space Structures," *Progress in Aeronautics and Astronautics,* Vol. 71, ed. H.B. Garrett and C.P. Pike, 1980, pp. 477-522.
[24]Whipple, E.C., "The Equilibrium Electric Potentials of a Body in the Upper Atmosphere and in Interplantary Space," Dissertation, George Washington Univ., Washington, D.C., 1965.
[25]Samir, U., "A Possible Explanation of an Order of Magnitude Discrepancy in Electron-Wake Measurements," *Journal of Geophysical Research,* Vol. 75, 1970, p. 855.
[26]Al'pert, J.L., Gurevic, A.V., and Pitaevsky, L.P., "Effects Due to an Artificial Satellite in Rapid Motion Through the Ionosphere or the Interplanetary Medium," *Space Science Reviews,* Vol. 2, 1963, p. 680.
[27]Katz, I., Parks, D.E., Mandell, M.J., Harvey, J.M., Brownell, Wang, S.S., and Rotenberg, M., "A Three Dimensional Dynamical Study of Electrostatic Charging in Materials," NASA CR-135256, 1977.
[28]Scheid, F., *Schaum's Outline Series: Theory and Problems of Numerical Analysis,* McGraw-Hill Book Co., New York, 1968.